Numerical simulation research on Sodium Laser Beacon imagings through the atmosphere turbulence

LIU Xiangyuan[1], QIAN Xianmei[2], ZHANG Suimeng[1], ZHAO Minfu[1], CUI Chaolong[2], HUANG Honghua[2]

(1. School of Materials and Chemical Engineering, West Anhui University, Lu'an, 237012, China；
2. Key Laboratory of Atmospheric Composition and Optical Radiation, Anhui Institute of Optics and Fine Mechanics, Chinese Academy of Sciences, Hefei, 230031, China)

Abstract: Based on the relative intensity distributions of Sodium Laser Beacon (SLB) and analysis of the on-axis imaging of incoherent light, considering the effects of atmospheric turbulence and the changes of **telescope** receiving diameter on the short-exposure SLB imgings on the focal plane, imagings of an extended source SLB are simulated under the three atmospheric turbulence models. Results indicate that sharpness and peak strehl ratio of SLB imagings increase but sharpness radius decrease with the **decrease** of atmosphere turbulence **strengths**. Moreover, the changes of telescope diameter from 3.0m to 1.5m cause the decrease of sharpness and peak strehl ratio but the increase of sharpness radius.

Key words: Sodium Laser Beacon; short-exposure imagings; relative intensity distributions; extended source

1 Introduction

Sodium Laser Beacon（SLB）is a man-made light source which is applied in adaptive optics. It is produced by fluorescence resonance of laser interacting with sodium atoms in the mesosphere. The light from SLB belongs to incoherent light. Its imaging can not be achieved by the coherent superposition of complex amplitude but can be done by the incoherent weighted superposition of point spread function (PSF) [1] . The ideal SLB is a point source. But the experimental researches show that SLBs always have a certain size due to effects of the turbulence, absorption and scattering of atmosphere. Jelonek et al[2]. applied the macro-micropulse laser to excite SLB. The average FWHW of SLB imagings is about 6.6 arcsec. Shi[3] achieved the FWHM of SLB 1.09 arcsec by using pulse laser in his experiments. Ge et al[4] got the samllest SLB whose FWHW is 0.8arcsec by using the continuous-wave(CW) laser with power 1W. Fugate et al[5] reported the three sky tests on SLB excitation with CW 8.5-W and 5.5-W laser at the Starfire Optical Range. Experiments indicate that the size of SLB excited by the circularly polarized laser is 1.15arcsec and by the linearly polarized laser is 2.16arcsec through the CCD camera images. Therefore, in fact, SLB can not be simply regarded as a point source.

The intend of this paper is to simulate and analyze the imaging of SLB on the focal plane through the atmospheric turbulence. Thus, in section 2, the theoretical models of incoherent imaging **are** analyzed and the numerical simulation methods are represented. In section 3, we focus on the short-exposure imgings of SLB under the three atmospheric turbulence models. The optical quality of SLB imagings is calculated. In section 4, we research on the sharpness, sharpness radius and peak strehl ratio of the short-exposure imgings of SLB on the focal plane when the telescope receiving diameters are 1.5m and 3.0m. Finally, in section 5, a few significative conclusions are made.

2 Theoretical models and numerical methods

The telescope can be regarded as an optical system with a single lens and aperture filter when it is used to observe the imgings of SLB. To facilitate the analysis, we assume that laser launch and telescope are on-axis. The telescope is a tye of Cassegrain. So, the intensity distribution of SLB on the focal plane is denoted as follows

$$\mathrm{I}_i(x_i, y_i) = \mathrm{I}_\mathrm{o}(x_\mathrm{o}, y_\mathrm{o}) \otimes \mathrm{h}_\mathrm{I}(x_\mathrm{o}, y_\mathrm{o}; x_i, y_i) \qquad (1)$$

Where, $\mathrm{I}_i(x_i, y_i)$ is the intensity distribution of SLB imagings, $\mathrm{I}_\mathrm{o}(x_\mathrm{o}, y_\mathrm{o})$ is the intensity distribution of SLB in the mesosphere, $\mathrm{h}_\mathrm{I}(x_\mathrm{o}, y_\mathrm{o}; x_i, y_i)$ is the incoherent PSF, $\otimes$ denotes convolution. Applying relation between convolution and Fourier transform, we obtain

This work was supported by the College Natural Science Foundation of Anhui Province, China (No. KJ2013A260)
Author, E-mail：lxy0564@aliyun.com，tele:18712376592

Selected Papers of the Photoelectronic Technology Committee Conferences held November 2015, edited by Yueguang Lv, Weimin Bao, Proc. of SPIE Vol. 9796, 979606 · © 2016 SPIE · CCC code: 0277-786X/16/$18 · doi: 10.1117/12.2228596

$$\mathrm{F}\left\{\mathrm{I}_i(x_i,y_i)\right\}=\mathrm{F}\left\{\mathrm{I}_{\mathrm{o}}(x_{\mathrm{o}},y_{\mathrm{o}})\right\}\mathrm{F}\left\{\mathrm{h}_{\mathrm{I}}(x_{\mathrm{o}},y_{\mathrm{o}};x_i,y_i)\right\} \quad (2)$$

Eq.(2) shows that the Fourier transform of $\mathrm{I}_i(x_i,y_i)$ depends on that of $\mathrm{h}_{\mathrm{I}}(x_{\mathrm{o}},y_{\mathrm{o}};x_i,y_i)$ under the known $\mathrm{I}_{\mathrm{o}}(x_{\mathrm{o}},y_{\mathrm{o}})$, that is

$$\begin{aligned}\mathrm{F}\left\{\mathrm{h}_{\mathrm{I}}(x_{\mathrm{o}},y_{\mathrm{o}};x_i,y_i)\right\}&=\mathrm{F}\left(\left|\mathrm{h}(x_i,y_i)\right|^2\right)\\&=\mathrm{F}\left\{\left|\mathrm{F}\left(\mathrm{P}(x,y)\exp[-j\Phi(x,y)]\right)\right|^2\right\}\end{aligned} \quad (3)$$

Where, $\mathrm{P}(x,y)$ is the pupil function which is 1 in the pupil and 0 out of the pupil, $\Phi(x,y)$ is the phase fluctuation caused by the atmospheric turbulence. Eq.(3) shows that the Fourier transform of $\mathrm{h}_{\mathrm{I}}(x_{\mathrm{o}},y_{\mathrm{o}};x_i,y_i)$ depends on $\mathrm{P}(x,y)$ and $\Phi(x,y)$.

For the $\mathrm{I}_{\mathrm{o}}(x_{\mathrm{o}},y_{\mathrm{o}})$, considering the intensity distributions of the laser transmission to the mesosphere, the number of the radiative photons in backscatter φ can be calculated. The express is given by

$$\varphi=\beta'\mathrm{C}_{\mathrm{Na}}\sum_i\Delta S_i\psi_i\mathrm{I}_i \quad (4)$$

In Eq.(4), β' is the backscatter coefficient of return photons, taking $\beta'=1.5$ for laser with circular polarization. ΔS_i is the very small area illuminated by laser. C_{Na} is the column density of sodium layer, taking $\mathrm{C}_{\mathrm{Na}}=4.0\times10^4$ atoms/cm^2, ψ_i is the average return photon flux, I_i is the intensity distribution of the incident laser in the mesosph -ere. When the CW laser interacts with sodium layer, the down-pumping, recoil and geomagnetic field often can affect the number of the radiative photons from SLB. In these aspects, Holzlöhner[6] and Rochester[7] detailedly study their change laws and gave LGSBloch package in Mathematica. One can set up a series of parameters including polarization, bandwidth, the angle between direction of laser beam and geomagnetic field etc to get $\psi_i(\mathrm{I})$. I is the independent variable which represents the intensity of incedent laser every point in the mesosphere.

Here, we set up the laser polarization is circular, laser bandwidth is 1MHz, the angle is 30$^{\mathrm{o}}$. By running LGSBloch software and fittings data, the $\psi_i(\mathrm{I})$ is obtained as follows.

$$\begin{aligned}\psi_i(\mathrm{I})=\;&0.09191g(\log_{10}\mathrm{I})^9+0.01142g(\log_{10}\mathrm{I})^8-1.663g(\log_{10}\mathrm{I})^7\\&-1.938g(\log_{10}\mathrm{I})^6+11.85g(\log_{10}\mathrm{I})^5+23.46g(\log_{10}\mathrm{I})^4\\&-35.33g(\log_{10}\mathrm{I})^3-104.2g(\log_{10}\mathrm{I})^2\\&-5.239g(\log_{10}\mathrm{I})+332.1\\&\mathrm{I}\in[0.01,1000]\ (\mathrm{W}/\mathrm{m}^2)\end{aligned} \quad (5)$$

Assuming that laser launch and telescope receiving systems are on-axis and laser is launched vertically, according to Eqs.(4) and (5), the number of return photons on the telescope receiving plane per unit area and time is

$$\Phi=\mathrm{T}_0\varphi/\mathrm{L}^2 \quad (6)$$

Where, T_0 is the atmospheric transmittance, taking $\mathrm{T}_0=0.84$, L is the altitude from the telescope plane to the sodium layer center, taking $\mathrm{L}=92\mathrm{km}$. According to Eqs.（5）and (6), the intensity distribution of SLB in the mesosphere is denoted by

$$\mathrm{I}(m,n)=\mathrm{T}_0\beta'\mathrm{C}_{\mathrm{Na}}\Delta S\psi_i(\mathrm{I})\mathrm{I}\bullet h\nu/\mathrm{L}^2 \quad (7)$$

In Eq. (7), $h\nu$ is the energy of a photon from the backscatter radiation of SLB. When the I is known, $\mathrm{I}(m,n)$ will be obtained. In Eq. (1), $\mathrm{I}_{\mathrm{o}}(x_{\mathrm{o}},y_{\mathrm{o}})$ is substituted by $\mathrm{I}(m,n)$. Nevertheless, $\mathrm{I}(m,n)$ denotes the relative intensity distribution of SLB in the case of the given conditions. First, the absorption and scattering of atmosphere only

cause the magnitude change of intensity instead of its distributions. Second, this intensity distribution is relative to the ground telescope with a given receiving diameter. This ground optical system can offer the adequate resolution. Third, assuming that the intensity distributions of SLB don't suffer the effects of atmospheric turbulence along the direction of downward light and there is no aberration in the optical system. According to the above all analysis, simulations of SLB imagings are summarized as follows.

1)The relative intensity distribution of SLB in the mesosphere, $\mathrm{I}_{\mathrm{o}}(x_{\mathrm{o}}, y_{\mathrm{o}})$, is simulated according to Eqs. (4) ~ (7). Then, $\mathrm{F}\{\mathrm{I}_{\mathrm{o}}(x_{\mathrm{o}}, y_{\mathrm{o}})\}$ is calculated.

2)The turbulence-indeced phase $\Phi(x, y)$, substituted by $\Phi(m, n)$, is generated by Kolmogorov Spectrum under three atmospheric turbulent models: HV5/7, Greenwood and ModHV models. Here, we will divide the atmospheric altitude into 20 segments. The different phase screens are generated at every segment. Then, they are added up as the phase fluctuation of the whole atmosphere.

3)The Fourier transform of the incoherent PSF, $\mathrm{F}\{\mathrm{h}_{\mathrm{I}}(x_{\mathrm{o}}, y_{\mathrm{o}}; x_i, y_i)\}$, is achieved according to Eq. (3).

4)By the inverse Fourier transform for $\mathrm{F}\{\mathrm{I}_i(x_i, y_i)\}$, the intensity distributions of SLB imagings on the focal plane are obtained according to Eq. (2).

3 Results and analysis

When laser launch and telescope are on-axis, SLB looks like an irregular disk from the backward observation. Besides the above simulated steps, the following problems also must be considered.

1)The size of the multi-phase screens should be more than the diameter of the optical system. Here, we take 3.0 meters as the diameter of telescope and set the number of phase screen grids 512×512 with grid interval 6mm. The Rytov index is same between two adjacent phase screens[8]. The simulation methods of phase screen proposed by Harding et al [9] are introduced.

2)The CW laser is a Gaussian beam with power 20W. The diameter of laser launch is 40cm. The beam quality factor is 1.1 and laser is launched vertically and in collimation. Then, the relative intensity distributions of SLB are simulated .

3)It is assumed that the tip-tilt of SLB would have been compensated, the dithering and wander of SLB imagings needn't be taken into account.

4)The area of circular telescope should remove the block area of laser launch. Thus, the pupil of telescope actually is annular.

5)The same PSF is used in the same isoplanatic angle under the same atmospheric turbulence model. The table 1 gives the different isoplanatic angles and radius covered by the same PSF under the HV5/7, Greenwood and ModHV models for atmospheric turbulence.

Table 1 Three atmosphere turbulence models , isoplanatic angles and radius covered by the same Point Spread Function (PSF)

Atmospheric turbulence models	Isoplanatic angles (rad)	Radius covered by the same PSF(m)
HV5/7	8.40×10^{-6}	0.773
Greenwood	1.67×10^{-5}	1.54
ModHV	2.14×10^{-5}	1.97

It can be seen from table 1 that the same PSF sufficiently covers the whole phase screen under the Greenwood and ModHV models for atmospheric turbulence, but it doesn't do under the HV5/7 model due to the samller isoplanatic angle. Therefore, it is necessary to introduce several PSFs for simulations of the SLB imgings. Here, the intensity distribution of every SLB is segmented into 4 parts and every part corresponds to the different PSF. Each time, the four imagings are added up to achieve the whole imaging after simulations for every part.

Based on the above considerations, figures 1 ~ 3 simulate the SLB imagings on the focal plane by the intensity

distributions. Every figure is one of random samlpes in all 25 times. The color bars in the right sides denote the magnitude of intensity in W/m^2.

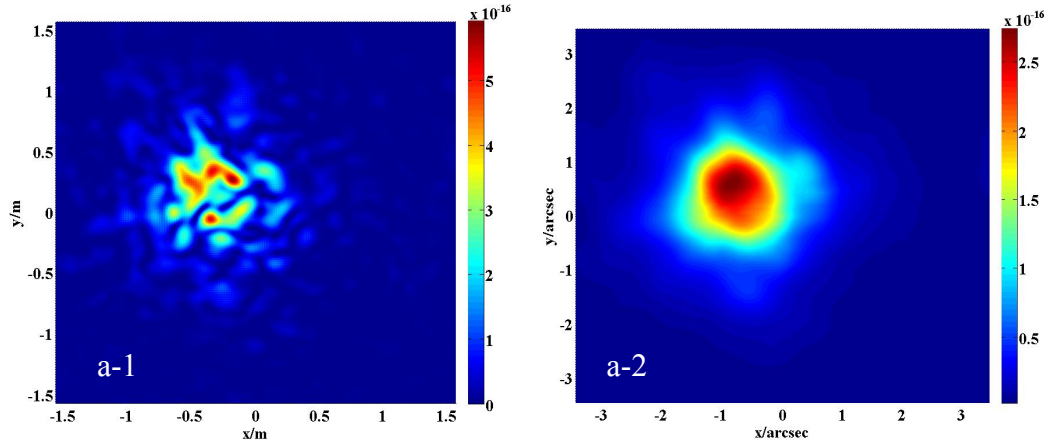

Fig. 1. (a-1)The relative intensity distribution of Sodium Laser Beacon in the mesosphere and (a-2)the imaging on the focal plane under the HV5/7 model for atmospheric turbulence.

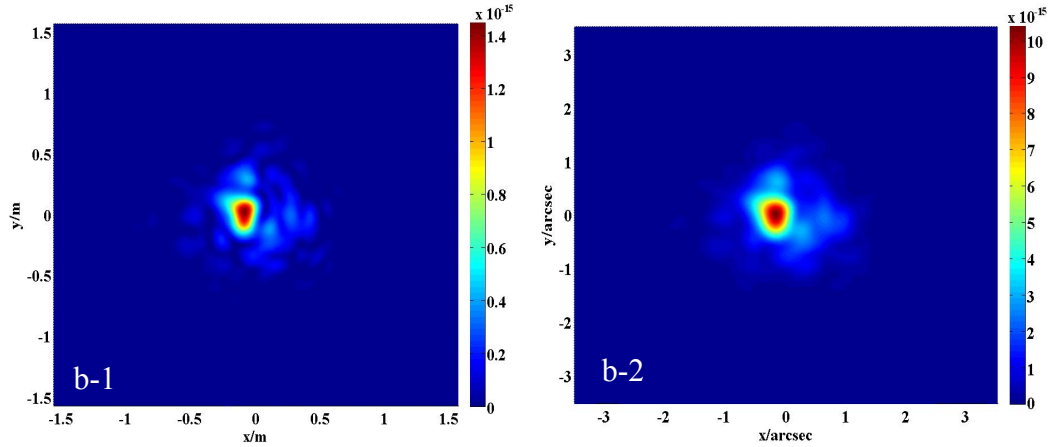

Fig. 2. (b-1)The relative intensity distribution of Sodium Laser Beacon in the mesosphere and (b-2)the imaging on the focal plane under the Greenwood model for atmospheric turbulence.

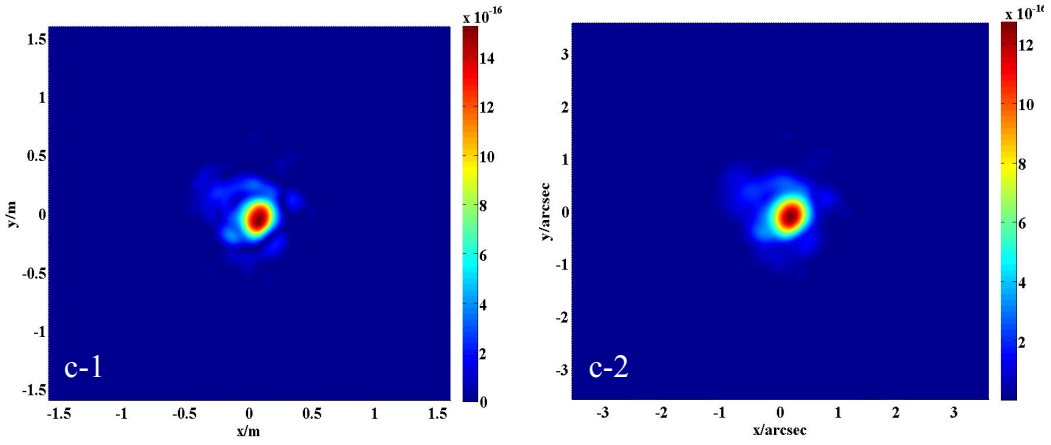

Fig. 3. (c-1)The relative intensity distribution of Sodium Laser Beacon in the mesosphere and (c-2)the imaging on the focal plane under the ModHV model for atmospheric turbulence.

From the above figures, one can see that the SLB imgings are obviously affected by atmospheric turbulence. The characters of imagings are very similar to the imagings of planets observed by Gaspard Duchên[10] and Gavel et al[11]. Although the relative intensity distribution of SLB itself is cracked in figure a-1, the imaging on the focal plane is combined into a body in figure a-2. Figures b-1 and c-1 are respectively the relative intensity distribution of SLB under the Greenwood and ModHV model for atmospheric turbulence. Comparing figures b-2 and c-2 with figure a-2, because the strength of atmospheric turbulence is stronger under the HV5/7 model, SLB imgings distinctly become blurred. Because the turbulent strength under the Greenwood model is relatively stronger than that under the ModHV model, the imaging in figure b-2 has more changes than that in figure c-2. Besides, the radius of SLB imagings under the HV5/7 model is bigger than that of the other two cases.

To quantitatively study the optical quality of SLB imagings and the energy focusability, sharpness（SP） is cited as a standard used in measurement[12]. The express is given by

$$\mathrm{SP} = \iint \mathrm{I}_i^2(x, y)dxdy \Big/ \iint \mathrm{I}_\mathrm{o}^2(x, y)dxdy \tag{8}$$

Where， $\mathrm{I}_i(x,y)$ is the intensity distribution of SLB imagings through atmospheric turbulence. $\mathrm{I}_\mathrm{o}(x,y)$ is the intensity distributions of SLB imagings without atmospheric turbulence. The sharpness is expressed in a discrete form as follows.

$$\mathrm{SP} = \sum_m \sum_n \mathrm{I}_i^2(m,n) \Big/ \sum_m \sum_n \mathrm{I}_\mathrm{o}^2(m,n) \tag{9}$$

Besides sharpness, the sharpness **radius**, $\mathrm{R}_{\mathrm{sh}}^2$, and the peak strehl ratio, S_{R0}, also can denote the optical quality, their expresses are respectively given below.

$$\mathrm{R}_{sh}^2 = 4\sum_m \sum_n r_i^2 \mathrm{I}_i^2(m,n) \Big/ \sum_m \sum_n \mathrm{I}_i^2(m,n) \tag{10}$$

$$\mathrm{S}_{\mathrm{R0}} = \mathrm{I}_{i\max} / \mathrm{I}_{\mathrm{o}\max} \tag{11}$$

In Eq. (10) and (11), r_i is the distance from the point $\mathrm{I}_i(m,n)$ to the centroid of SLB spot. Therefore, before calculating the sharpness, the centroid place should first be known. $\mathrm{I}_{i\max}$ denotes the peak intensity of SLB imagings through atmospheric turbulence. $\mathrm{I}_{\mathrm{o}\max}$ denotes the peak intensity of SLB imagings without atmospheric turbulence, $\mathrm{I}_\mathrm{o}(x,y)$.

We apply Eqs. (9) ~ (11) to calculate sharpness, sharpness radius and peak strehl ratio of SLB imagings under the three atmospheric turbulence models 25 times. The average values of 25 times are listed in table 2 where r_0 the Fried's parameters in the vertical direction corresponding to the wavelength 589 nm.

Table.2 Average values of sharpness, sharpness radius and peak strehl ratio on the focal plane under the three atmospheric turbulence models.

Atmospheric turbulence models	HV5/7 model r_0 =6cm	Greenwood model r_0 =15.5cm	ModHV model r_0 =21.8cm
Sharpness (SP)	0.5997	0.7374	0.7932
Sharpness radius （$\mathrm{R}_{\mathrm{sh}}^2/\mathrm{m}^2$）	0.7736	0.1883	0.1189
Peak strehl ratio (S_{R0})	0.4631	0.7094	0.8114

From table 2, one can see that sharpness and peak strehl ratio of SLB imagings have an increase tendency with the increase of Fried's parameters. The sharpness radius has a decrease tendency. These results are identical with pepole's recognization about effects of atmospheric turbulence on imagings.

Under the HV5/7 model for atmospheric turbulence, the numerical simulation results of figure 1 use 4 PSFs. If one PSF is used, the following figure 4 will be obtained.

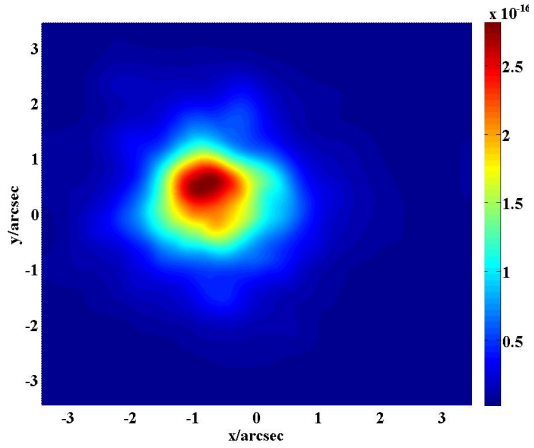

Fig. 4. Imaging on the imaging plane simulated by one Point Spread Function under the HV5/7 model for atmospheric turbulence .

Comparing figure 4 with figure a-2, there is a certain difference between the two from their appearances. The intensity distribution of figure 4 is slightly concentration. Calculation results show that the peak strehl ratio of SLB in figure a-2 is $S_{R0} = 0.4631$ and that of SLB in figure 4 is $S_{R0} = 0.4757$. However, under the HV5/7 model for atmospheric turbulence, using one PSF to simulate the SLB imagings does not accord with reality.

4 Effects of the telescope diameter changes on imagings

The telescope diameter is regarded as the size of pupil in the above research. In order to explore the influence of telescope diameter(TD) changes on the short-exposure SLB imgings, the telescope diameter becomes 1.5m in the case of the laser launch diameter unchanged. Thus, the loss of downward light from SLB roughly is 7% due to the block of laser launch. When the other parameters are fixed, figures 5 ~ 7 simulate the SLB imagings on the focal plane under the three atmospheric turbulence models. The color bars denote the magnitude of intensity in W/m^2.

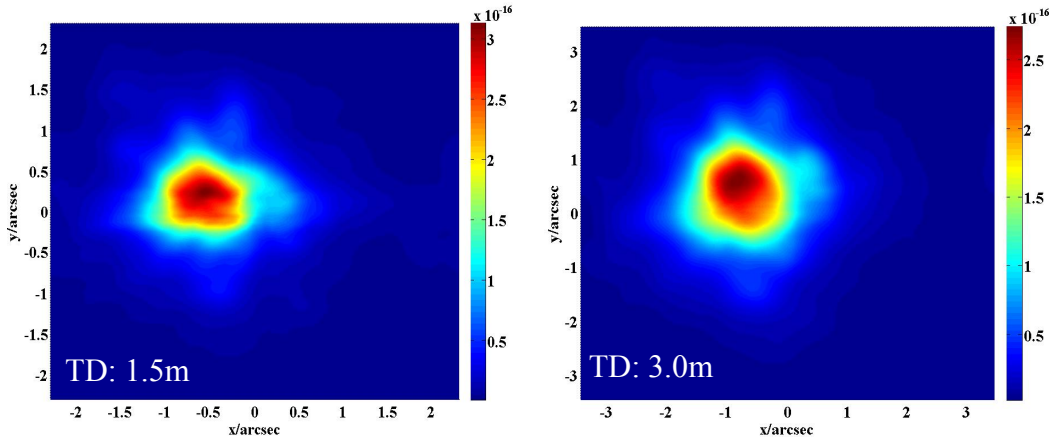

Fig.5. (left)Imaging of Sodium Laser Beacon by 1.5m telescope diameter and (right) by 3.0m telescope diameter on the focal plane under the HV5/7 model for atmospheric turbulence.

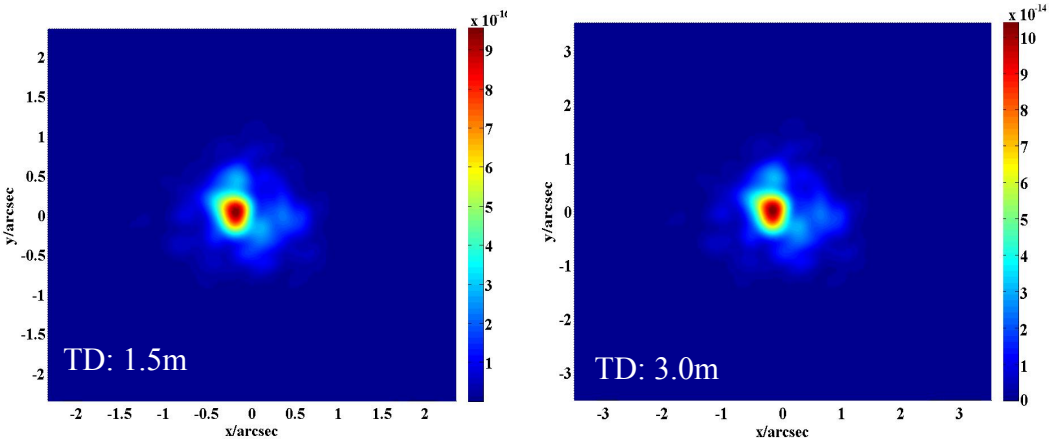

Fig.6. (left)Imaging of Sodium Laser Beacon by 1.5m telescope diameter and (right) by 3.0m telescope diameter on the focal plane under the Greenwood model for atmospheric turbulence.

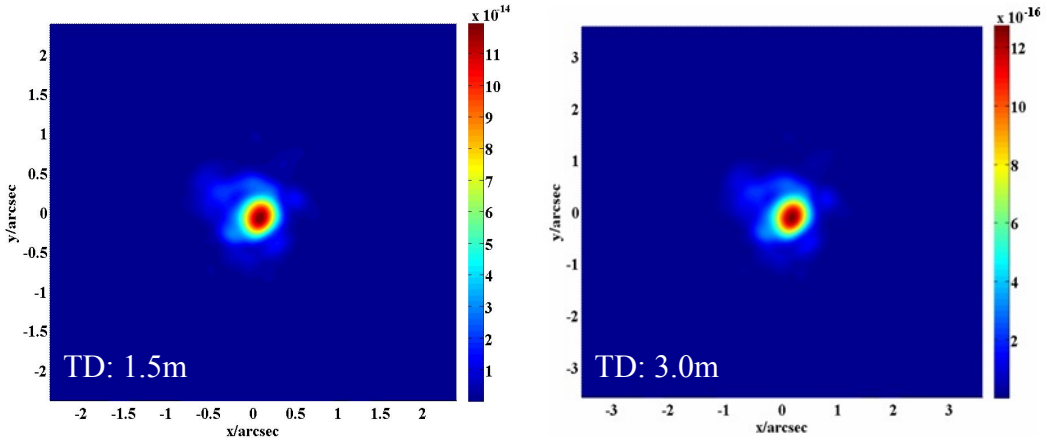

Fig.7. (left)Imaging of Sodium Laser Beacon by 1.5m telescope diameter and (right) by 3.0m telescope diameter on the focal plane under the ModHV model for atmospheric turbulence.

From figures 5 to 7, except for view field and magnitude of intensity, the changes of telescope diameter from 3.0m to 1.5m don't have a great effect on the SLB imagings. Comparatively, the SLB imagings have more distinct changes under the HV5/7 model for atmospheric turbulence than under the other two models from their appearances. For the 1.5m telescope diameter, sharpness, peak strehl ratio and sharpness radius of SLB imagings are calculated under the three atmospheric turbulence models. These average values of 25 times are listed in table 3.

Table.3 The average values of sharpness, sharpness radius and peak strehl ratio on the focal plane under the three atmospheric turbulence models by 1.5m diamter

Models for atmospheric turbulence	HV5/7 model r_0 =6cm	Greenwood model r_0 =15.5cm	ModHV model r_0 =21.8cm
Sharpness (SP)	0.5403	0.6592	0.6980
Sharpness radius (R_{sh}^2/m^2)	0.7857	0.1890	0.1201
Peak strehl ratio (S_{R0})	0.4274	0.6613	0.7581

Comparing table 3 with table 2, the sharpness, peak strehl ratio and sharpness radius of SLB imagings in **the** case of telescope diameter being 1.5m and 3.0m have a similar change tendency **with the decrease of atmosphere turbulence strengths**. But the sharpness, peak strehl ratio of SLB imagings decrease and the sharpness radius slightly increase when the **telescope diameters changes from 3.0m to 1.5m.**

5 Conclusions

This article regards SLB as an incoherent and extended source. Based on the theory of on-axis imagings and the relative intensity distributions of SLB, effects of the telescope diameter and atmospheric turbulence on the short-exposure imgings of SLB are simulated and analyzed. The sharpness, peak strehl ratio and sharpness radius of SLB imagings are calculated under the three atmospheric turbulent models. We make some conclsions as follows.

1)The isoplanatic angle should be considered when SLB imagings is simulated. If the size of SLB is beyond the scale covered by the one SPF, several different SPFs should be adopted. Thus, results accord with reality.

2)Atmospheric turbulence and the changes of telescope diameter influence on the SLB imagings. When the strength of atmospheric turbulence is stronger, the sharpness and peak strehl ratio of SLB imagings decrease and the sharpness radius increases. When the telescope diameter reduces from 3.0m to 1.5m, a similar change will also happen.

In conclusion, when SLB imagings being simulated , SLB should be regarded as an incoherent and extended source. The magnitude of isoplanatic angle and effects of atmospheric turbulence as well as the changes of telescope diameter should be considered.

References

[1]Joseph W. Goodman, [Introduction to Fourier Optics], McGraw-Hill Companies, INC, **New York**, 100-150(1996)

[2]Jelonek M. P., Fugate R. Q., Lange W. J., et al., “Characterization of artificial guide stars generated in the mesospheric sodium layer with a sum-frequency laser, ” J. Opt. Soc. Am. A, **11**(2): 806-812 (1994)

[3]Shi F., “Sodium Laser Guide Star Experiment with a Sum-Frequency Laser for Adaptive Optics,” Publications of the Astronomical Society of the Pacific, **113**: 366–378(2001)

[4]Ge J., Jacobsen B. P., Angela J.R.P., et al., “Sodium Laser Guide Star Brightness, Spot size, and Sodium Layer Abundance, ” SPIE Proc., **3353**: 242(1998)

[5]Fugate R. Q., Denman C A., Hilman P. D., et al.,“Progress toward a 50-watt facility-class sodium guidestar pump laser, ” Proc. SPIE, **5490** : 1010-1020(2004)

[6]Holzlöhner R., Rochester S. M., Calia D. B., et. al., “Optimization of cw sodium laser guide star efficiency, ” Astronomy & Astrophysics, **510**: 1-14(2010)

[7] Rochester S.M., A.Otarola, Boyer C., et al., “Modeling of pulsed laser guide stars for the Thirty Meter Telescope project, ” J.Opt. Soc.Am.A, **6**(19): 832-845(2012)

[8]Qian X., Zhu W., Rao R., “Phase screen distribution for simulating laser propagation along an inhomogeneous atmospheric path (in Chinese), ” Acta Physics Sinica, **58** : 6633-6639(2009)

[9]Harding C. D., Johnston R. A., Lane R. G., “Fast simulation of Kolmogorov phase screen,” Appl. Opt., **38**(11): 2161-2170(1999)

[10]Gaspard D., “High-angular resolution imaging of disks and planets,” New Astronomy Reviews, **52** (4): 117-144(2008)

[11]Gavel D. T., Gates E. L., Max C. E., et al., “Recent science and engineering results with the laser guidestar adaptive optics system at Lick Observatory, ” Proc. SPIE, **4839**: 354-359(2003)

[12]Muller R. A., Buffington A., “Real-time correction of atmospherically degraded telescope images through image sharpening , ” J. Opt. Soc. Am., **64**:1200–1210 (1974)